Here are the proofs of your article.

- You can submit your corrections online, via e-mail or by fax.
- For **online** submission please insert your corrections in the online correction form. Always indicate the line number to which the correction refers.
- You can also insert your corrections in the proof PDF and email the annotated PDF.
- For fax submission, please ensure that your corrections are clearly legible. Use a fine black pen and write the correction in the margin, not too close to the edge of the page.
- Remember to note the **journal title**, **article number**, and **your name** when sending your response via e-mail or fax.
- Check the metadata sheet to make sure that the header information, especially author names and the corresponding affiliations are correctly shown.
- Check the questions that may have arisen during copy editing and insert your answers/ corrections.
- **Check** that the text is complete and that all figures, tables and their legends are included. Also check the accuracy of special characters, equations, and electronic supplementary material if applicable. If necessary refer to the *Edited manuscript*.
- The publication of inaccurate data such as dosages and units can have serious consequences. Please take particular care that all such details are correct.
- Please do not make changes that involve only matters of style. We have generally introduced forms that follow the journal's style.
 Substantial changes in content, e.g., new results, corrected values, title and authorship are not allowed without the approval of the responsible editor. In such a case, please contact the Editorial Office and return his/her consent together with the proof.
- If we do not receive your corrections within 48 hours, we will send you a reminder.
- Your article will be published **Online First** approximately one week after receipt of your corrected proofs. This is the **official first publication** citable with the DOI. **Further changes** are, therefore, not possible.
- The **printed version** will follow in a forthcoming issue.

Please note

After online publication, subscribers (personal/institutional) to this journal will have access to the complete article via the DOI using the URL: http://dx.doi.org/[DOI].

If you would like to know when your article has been published online, take advantage of our free alert service. For registration and further information go to: http://www.link.springer.com.

Due to the electronic nature of the procedure, the manuscript and the original figures will only be returned to you on special request. When you return your corrections, please inform us if you would like to have these documents returned.

Metadata of the article that will be visualized in OnlineFirst

ArticleTitle	Strain-Insensitive Hierarchically Structured Stretchable Microstrip Antennas for Robust Wireless Communication		
Article Sub-Title			
Article CopyRight	The Author(s) (This will be the copyright line in the final PDF)		
Journal Name	Nano-Micro Letters		
Corresponding Author	Family Name	Zhu	
	Particle		
	Given Name	Jia	
	Suffix		
	Division	Department of Engineering Science and Mechanics	
	Organization	The Pennsylvania State University	
	Address	University Park, PA, 16802, USA	
	Phone		
	Fax		
	Email	jmz5364@psu.edu	
	URL		
	ORCID		
Corresponding Author	Family Name	Cheng	
1 0	Particle		
	Given Name	Huanyu	
	Suffix		
	Division	Department of Engineering Science and Mechanics	
	Organization	The Pennsylvania State University	
	Address	University Park, PA, 16802, USA	
	Division	Department of Materials Science and Engineering	
	Organization	The Pennsylvania State University	
	Address	University Park, PA, 16802, USA	
	Phone		
	Fax		
	Email	Huanyu.Cheng@psu.edu	
	URL		
	ORCID		
Author	Family Name	Zhang	
	Particle		
	Given Name	Senhao	
	Suffix		
	Division	Department of Engineering Science and Mechanics	
	Organization	The Pennsylvania State University	
	Address	University Park, PA, 16802, USA	

	Division	Division of Life Sciences and Medicine, School of Biomedical Engineering (Suzhou)
	Organization	University of Science and Technology of China
	Address	Hefei, 230022, People's Republic of China
	Division	Institute of Biomedical Engineering and Technology
	Organization	Chinese Academy of Science
	Address	Suzhou, 215011, People's Republic of China
	Phone	
	Fax	
	Email	
	URL	
	ORCID	
Author	Family Name	Yi
	Particle	
	Given Name	Ning
	Suffix	
	Division	Department of Materials Science and Engineering
	Organization	The Pennsylvania State University
	Address	University Park, PA, 16802, USA
	Phone	
	Fax	
	Email	
	URL	
	ORCID	
Author	Family Name	Song
	Particle	
	Given Name	Chaoyun
	Suffix	
	Division	School of Engineering and Physical Sciences
	Organization	Heriot-Watt University
	Address	University Park, Edinburgh, EH14 4AS, Scotland, UK
	Phone	
	Fax	
	Email	
	URL	
	ORCID	
Author	Family Name	Qiu
	Particle	
	Given Name	Donghai
	Suffix	
	Division	Institute of Biomedical Engineering and Technology
	Organization	Chinese Academy of Science
	Address	Suzhou, 215011, People's Republic of China
	Phone	
	Fax	

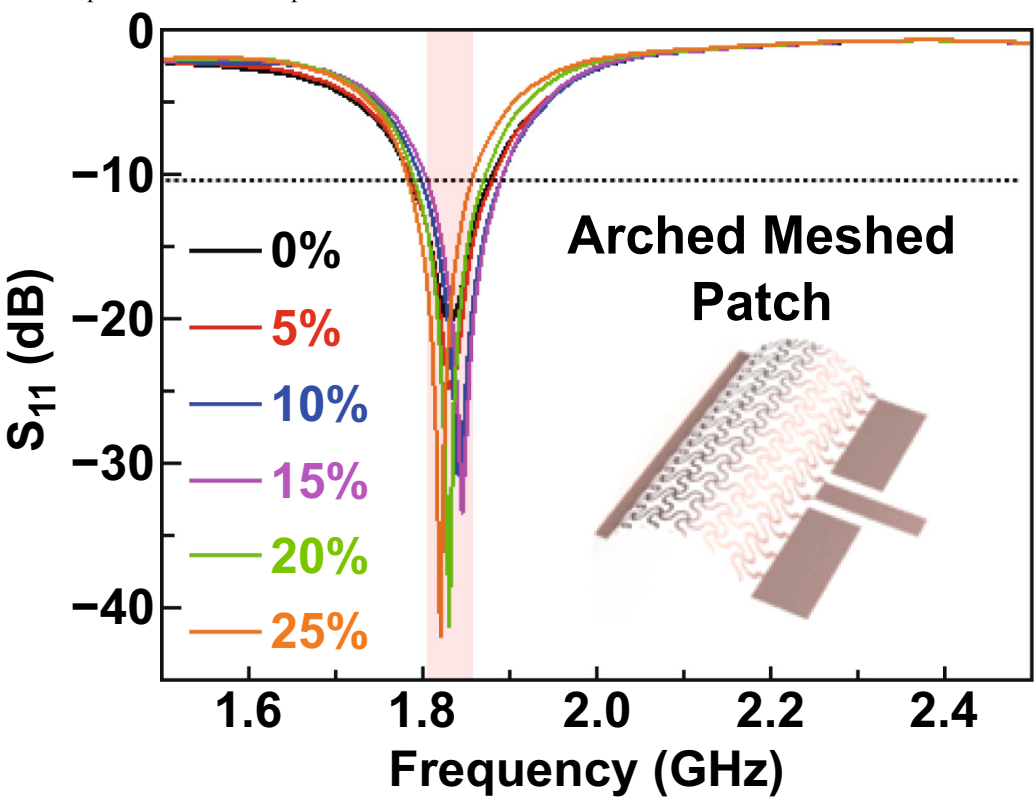
	Email	
	URL	
	ORCID	
Author	Family Name	Hu
	Particle	
	Given Name	Zhihui
	Suffix	
	Division	Department of Engineering Science and Mechanics
	Organization	The Pennsylvania State University
	Address	University Park, PA, 16802, USA
	Phone	
	Fax	
	Email	
	URL	
	ORCID	
Author	Family Name	Li
	Particle	
	Given Name	Bowen
	Suffix	
	Division	Department of Engineering Science and Mechanics
	Organization	The Pennsylvania State University
	Address	University Park, PA, 16802, USA
	Phone	
	Fax	
	Email	
	URL	
	ORCID	
Author	Family Name	Xing
	Particle	
	Given Name	Chenghao
	Suffix	
	Division	Department of Electrical Engineering
	Organization	The Pennsylvania State University
	Address	University Park, PA, 16802, USA
	Phone	
	Fax	
	Email	
	URL	
	ORCID	
Author	Family Name	Yang
	Particle	
	Given Name	Hongbo
	Suffix	
	Division	Division of Life Sciences and Medicine, School of Biomedical Engineering (Suzhou)

	Organization	University of Science and Technology of China
	Address	Hefei, 230022, People's Republic of China
	Division	Institute of Biomedical Engineering and Technology
	Organization	Chinese Academy of Science
	Address	Suzhou, 215011, People's Republic of China
	Phone	
	Fax	
	Email	
	URL	
	ORCID	
Author	Family Name	Wang
	Particle	
	Given Name	Qing
	Suffix	
	Division	Department of Materials Science and Engineering
	Organization	The Pennsylvania State University
	Address	University Park, PA, 16802, USA
	Phone	
	Fax	
	Email	
	URL	
	ORCID	
	Received	15 December 2020
Schedule	Revised	
	Accepted	23 February 2021
Highlights	The "ordered-unraveli	ng" of hierarchical structures from mechanical assembly contributes to not only the

The "ordered-unraveling" of hierarchical structures from mechanical assembly contributes to not only the improved overall stretchability, but also the small resonance shift of the stretchable microstrip antenna upon stretching. A double-arched microstrip antenna was demonstrated to communicate wirelessly upon 25% stretching or when being placed on human bodies.

As the key component of wireless data transmission and powering, stretchable antennas play an indispensable role in flexible/stretchable electronics. However, they often suffer from the frequency detuning upon mechanical deformations; thus, their applications are limited to wireless sensing with wireless transmission capabilities remained elusive. Here, a hierarchically structured stretchable microstrip antenna with meshed patterns arranged in an arched shape showcases tunable resonance frequency upon deformations with improved overall stretchability. The almost unchanged resonance frequency during deformations enables robust on-body wireless communication and RF energy harvesting, whereas the rapid changing resonance frequency with deformations allows for wireless sensing. The proposed stretchable microstrip antenna was demonstrated to communicate wirelessly with a transmitter (input power of -3 dBm) efficiently (i.e., the receiving power higher than -100 dBm over a distance of 100 m) on human bodies even upon 25% stretching. The flexibility in structural engineering combined with the coupled mechanical–electromagnetic simulations provides a versatile engineering toolkit to design stretchable

microstrip antennas and other potential wireless devices for stretchable electronics.



Keywords (separated by '-')	Stretchable microstrip antennas - Strain-insensitive resonance frequency - Wireless communication - RF energy harvesting - Wearable and bio-integrated electronics
Footnote Information	Jia Zhu and Senhao Zhang contributed equally to this study and share the first authorship. Supplementary Information The online version contains supplementary material available at (https://doi.org/10.1007/s40820-021-00631-5).

Journal: Large 40820 Article No: 631 MS Code : 631 Dispatch: 27-3-2021

Nano-Micro Letters

ISSN 2311-6706 e-ISSN 2150-5551 CN 31-2103/TB

ARTICLE

https://doi.org/10.1007/s40820-021-00631-

8

9

10

11

12 13

14

15

16

17

18

19

20

21

22

23

24

25

26

27

Α1

Α2

АЗ

Α4

Α5

Α8

A9

Cite as

Nano-Micro Lett.

Received: 15 December 2020 Accepted: 23 February 2021 © The Author(s) 2021

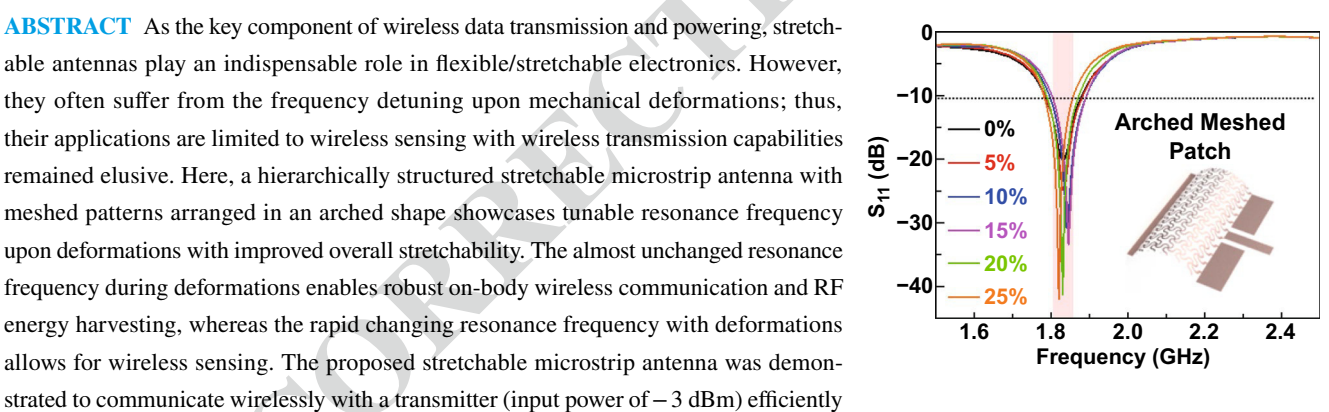
Strain-Insensitive Hierarchically Structured Stretchable Microstrip Antennas for Robust Wireless Communication

Jia Zhu^{1 ⊠}, Senhao Zhang^{1,2,3}, Ning Yi⁴, Chaoyun Song⁵, Donghai Qiu³, Zhihui Hu¹, Bowen Li¹, Chenghao Xing⁶, Hongbo Yang^{2,3}, Qing Wang⁴, Huanyu Cheng^{1,4}

HIGHLIGHTS

- The "ordered-unraveling" of hierarchical structures from mechanical assembly contributes to not only the improved overall stretchability, but also the small resonance shift of the stretchable microstrip antenna upon stretching.
- A double-arched microstrip antenna was demonstrated to communicate wirelessly upon 25% stretching or when being placed on human bodies.

ABSTRACT As the key component of wireless data transmission and powering, stretchable antennas play an indispensable role in flexible/stretchable electronics. However, they often suffer from the frequency detuning upon mechanical deformations; thus, their applications are limited to wireless sensing with wireless transmission capabilities remained elusive. Here, a hierarchically structured stretchable microstrip antenna with meshed patterns arranged in an arched shape showcases tunable resonance frequency upon deformations with improved overall stretchability. The almost unchanged resonance frequency during deformations enables robust on-body wireless communication and RF energy harvesting, whereas the rapid changing resonance frequency with deformations allows for wireless sensing. The proposed stretchable microstrip antenna was demon-



(i.e., the receiving power higher than - 100 dBm over a distance of 100 m) on human bodies even upon 25% stretching. The flexibility in structural engineering combined with the coupled mechanical-electromagnetic simulations provides a versatile engineering toolkit to design stretchable microstrip antennas and other potential wireless devices for stretchable electronics.

KEYWORDS Stretchable microstrip antennas; Strain-insensitive resonance frequency; Wireless communication; RF energy harvesting;

28 Wearable and bio-integrated electronics

Jia Zhu and Senhao Zhang contributed equally to this study and share the first authorship.

☑ Jia Zhu, jmz5364@psu.edu; Huanyu Cheng, Huanyu.Cheng@psu.edu

- Department of Engineering Science and Mechanics, The Pennsylvania State University, University Park, PA 16802, USA
- Division of Life Sciences and Medicine, School of Biomedical Engineering (Suzhou), University of Science and Technology of China, Hefei 230022, People's Republic of China
- Institute of Biomedical Engineering and Technology, Chinese Academy of Science, Suzhou 215011, People's Republic of China
- A6 Department of Materials Science and Engineering, The Pennsylvania State University, University Park, PA 16802, USA Α7
 - School of Engineering and Physical Sciences, Heriot-Watt University, University Park, Edinburgh EH14 4AS, Scotland, UK
 - Department of Electrical Engineering, The Pennsylvania State University, University Park, PA 16802, USA



Article No: 631

73

74

75

76

77

78

79

80

81

82

83

84

85

86

87

88

89

90

91

92

93

94

95

96

97

98

99

100

101

102

103

104

105

106

107

108

109

110

111

112

113

30

31

32

33

34

35

36

37

38

39

40

41

42

43

44

45

46

47

48

49

50

51

52

53

54

55

56

57

58

59

60

61

62

63

64

65

66

67

68

69

70

71

1 Introduction

Flexible/stretchable electronics attached to dynamically changing, curvilinear surfaces can still function properly upon various mechanical deformations, including stretching, bending, and twisting [1]. The integration of sensors and actuators with data communication and powering modules in this class of emerging electronics enables its applications in the energy generator/storage [2-6], human-machine interfaces [7, 8], health monitoring [9, 10], and clinical treatments [11]. The commonly used strategies in the design and fabrication of flexible/stretchable electronics rely on either intrinsically stretchable materials [12, 13] or stretchable structures [14-18]. The former includes the intrinsically stretchable semiconductors, insulators, and conductors. With direct relevance to wireless devices such as antennas, the intrinsically stretchable conductors often explore conductive polymers [19], liquid metals [20], and conductive composites with lowdimensional nanofillers in a stretchable polymeric matrix [21]. Alternatively, the latter stretchable structures (e.g., serpentine [22–24] or 3D structures [14–16, 25]) allow the conventional metals to be stretched over tens of percent without damage. Compared to the intrinsically stretchable materials with various functionalities, the conventional metal conductors (and semiconductors) with stretchable structures exhibit high performance comparable with modern electronics. Additionally, they can easily integrate the other commercial off-the-shelf (COTS) chips through a conventional soldering process to achieve extended capabilities for mass-production and commercialization.

As an indispensable component in flexible/stretchable electronics, wireless technology allows wireless powering [24] and data transmission [26-28] in the resulting miniaturized, integrated systems. For instance, near-field communication (NFC) has been widely used in wireless epidermal electronic systems [26] to monitor various physiologically relevant signals. However, its applications are limited by the short working distance. On the other hand, far-field communication with a radiofrequency (RF) antenna can be leveraged for wireless data and energy communication at a much longer working distance [10]. The combination of RF antenna and rectifying circuit results in a rectifying antenna (rectenna) to harvest ambient RF energies for low-power flexible/stretchable electronics [29, 30]. As a result, the development of stretchable antennas and rectennas starts to gain momentum recently. Compared to the dipole and loop antennas, the microstrip patch antennas showcase significantly improved on-bodies performance because the ground plane can help eliminate or reduce the effect from the underlying lossy tissues [31]. In contrast to stretchable antennas based on liquid metals [32–34], conductive textile [35], or conductive composites [36], the stretchable metal antennas exhibit enhanced radiation efficiency due to the low ohm loss.

The resonance frequency of stretchable antennas with either stretchable materials or structures shifts with tensile deformations, i.e., the frequency detuning [31, 32, 37, 38]. As a result, the stretchable antennas are only applied as wireless sensors based on the frequency shift [32, 38]. It is highly desirable to design stretchable antennas with strain-insensitive resonance frequency for robust wireless communication and RF energy harvesting. Although a stretchable monopole antenna with a relatively wide band has been demonstrated for communication, its radiation performance degrades when used on-body [39] because of the absence of a ground plane. Here, we report hierarchically structured stretchable microstrip antennas with meshed patch mechanically popped-up into a 3D shape to showcase the strain-insensitive resonance frequency over a large range of stretching up to 25%. The strain-insensitive resonance frequency comes from the cancellation of two effects, i.e., the increasing (or decreasing) resonance frequency of stretchable microstrip antennas with a meshed (or arched) patch as stretching increases, as revealed in our prior report [18]. The ground plane in the antenna also minimizes the effect from lossy human tissues when the antenna is used on-body [40, 41]. The resulting stretchable microstrip antenna with a strain-insensitive resonance demonstrates excellent on-body performance from wireless communication to RF energy harvesting.

2 Experimental Section

2.1 Measurement of Dielectric Properties of Elastomeric Substrates

The elastomeric Ecoflex substrates were fabricated by mixing parts A and B with a ratio of 1:1. After cured at room

157

158

159

160

161

162

163

164

165

166

167

168

169

170

171

172

173

174

175

176

177

178

179

180

181

182

183

184

185

186

187

188

189

190

191

192

193

114

115

116

117 118

119

120

121

122

123

124

125

126

127

128

129

130

131

132

133

134

135

136

137

138

139

140

141

142

143

144

145

146

147

148

149

150

151

152

153

154

155

temperature for 3 h, the Ecoflex samples in a square shape of 15 by 15 mm with a thickness of 1 mm were prepared for dielectric property measurements. A resonant mode dielectrometer (RMD-C-100, GDK Product Inc.) was used to measure the dielectric constant and loss tangent over the range from 1 to 10 GHz. Input microwaves from a vector network were used to interact with the cavity of the resonant mode dielectrometer. The shift in resonance mode and the corresponding quality factor between the measurements with and without the sample determined the dielectric constant and loss of the sample. The measurements indicated that the dielectric properties underwent a negligible change in the frequency range from 1 to 5 GHz. Therefore, the dielectric constant of 3.125 and loss tangent of 0.01 (at 2.4 GHz) were used for the Ecoflex substrate in the design of stretchable antennas. The good agreement between the simulated and measured resonance frequency

2.2 Fabrication of the Stretchable Microstrip Antennas

verified the accurate measurement of dielectric properties.

The meshed layout designed in the AutoCAD software was imported into the control system of an ultraviolet picosecond laser system (BX15, Edgewave). Commercial copper foils with a thickness of 20 µm (BangKai) fixed on a silicon wafer temporarily by the capillary force of water were patterned into the programmed mesh design by the laser system. The cutting power and speed of 0.4 µJ and 2000 mm s⁻¹ were optimized to achieve the best spatial resolution. A soft adhesive silicone gel (v1510, Valigoo) was used to assemble the patterned patch and ground onto the Ecoflex substrate in a rectangular shape of $50 \times 50 \text{ mm}^2$ with a thickness of 1.5 mm. Depending on the number of arches (i.e., single- or double-arched), the meshed patch and ground were selectively bonded to the prestrained Ecoflex substrate with a pre-strain of 5%, 10%, or 15%. The release of the pre-strain resulted in the arched microstrip antennas with arched patch and ground. When the selectively bonded ground was replaced by fully bonded ground, the stretchable antenna with an arched patch and a meshed ground was obtained. The meshed microstrip antenna was obtained by the fully bonding of the meshed serpentine patch and ground to the Ecoflex substrate without the pre-strain. Soldering the as-fabricated antennas with a SubMiniature version A (SMA) connector with a soldering iron (Sn42Bi58, KZ-1513) completed the fabrication process.

2.3 Measurement of Radiation Properties of Microstrip Antennas

The tensile strain in the range from 0 to 25% was applied to the stretchable microstrip antenna by a custom-built stretcher. Cylinders with different radii were used in the bending test of the antenna. The reflection curves (S_{11}) of the deformed microstrip antenna were measured by a vector network analyzer (T5260A, Transcom Instruments). The radiation patterns were measured in an anechoic chamber. The on-body performance of the antenna was measured by attaching it to the arm of a healthy human subject with Magic tapes.

2.4 Wireless Communication of the Stretchable Microstrip Antenna

The commercial RF evaluation kit (SmartRF06) was employed to measure the wireless communication performance of the stretchable microstrip antenna. Two boards integrated with the CC2538 RF chip act as the transmitter and receiver, respectively. The chip can be programmed to transmit the RF energy at a power of -3 dBm (0.50 mW). A PCB-based monopolar antenna was connected with the transmitter to provide omnidirectional radiation. The double-arched stretchable microstrip antenna resonating at 2.45 GHz was connected with the receiver to wirelessly communicate with the transmitter. The receiver was programmed to have a sensitivity of -100 dBm. The receiving power at different distances for the stretchable microstrip antenna placed in the free space or on the human skin with stretching was measured, respectively.

3 Results and Discussion

Stretchable structures such as horseshoe unit cells and arched elements have been explored to result in stretchable microstrip antennas with conventional metals. The combination of the two design strategies into the hierarchically structured microstrip antennas (Fig. 1a) provides improved





214

215

216

217

218

219

220

221

222

223

224

225

226

227

228

229

230

231

232

233

234

235

236

237

238

239

240

241

242

243

244

245

246

247

248

249

250

251

252

253

254

255

194

195

196

197

198

199

200

201

202

203

204

205

206

207

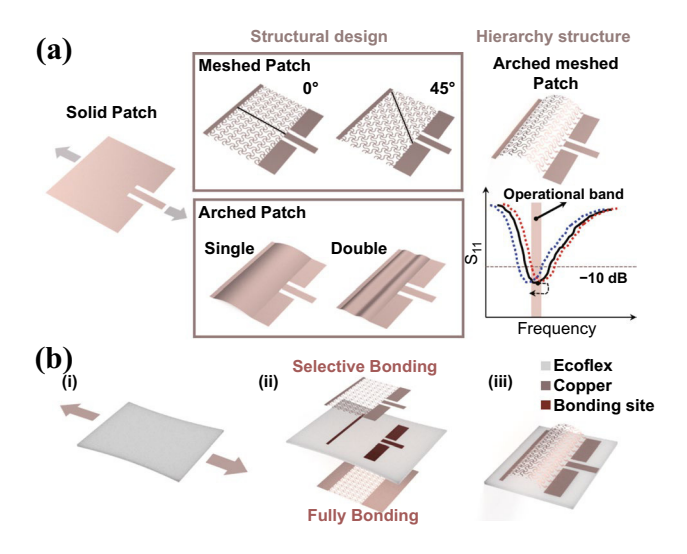
208

209

210

211

212



Article No: 631

Fig. 1 Schematic to demonstrate the design strategies of hierarchically structured stretchable microstrip antennas with horseshoe unit cells in a meshed layout and a 3D arched structure. a Design parameters in the stretchable structures include the orientation of the meshed layout and the number of 3D arches. In addition to an improved stretchability, the programmable mechanical-electromagnetic properties in the hierarchically structured stretchable microstrip antennas allow them to be strain-sensitive or strain-insensitive, with the former for wireless sensing and the latter for wireless communication and RF energy harvesting. b Fabrication process of the hierarchically structured antenna from the mechanical assembly. (i) After the soft Ecoflex substrate is pre-stretched, (ii) the meshed Cu structure patterned by laser is attached to the pre-stretched substrate with selective bonding sites, (iii) release of the pre-strain lifts the non-bonded region to form a 3D structure

stretchability and versatile tuning of mechanical-electromagnetic properties because of the programmed structure unfolding upon stretching. Mechanical assembly of the meshed metal patch and ground with horseshoe unit cells on a soft Ecoflex substrate (dielectric constant and loss tangent of 3.125 and 0.01) results in the stretchable microstrip antennas with hierarchical structures (Fig. 1b). Although the horseshoe unit cells with different characteristic dimensions can be arranged in a periodic lattice (e.g., rectangular, triangular, or hexagonal) [23], this study simply uses the anisotropic square lattice structure with different mesh orientations to demonstrate the design concept. In brief, the fabrication starts with the laser patterning of the meshed metal patch and ground with horseshoe unit cells. Next, the meshed metal patch and ground are selectively bonded to a pre-stretched Ecoflex substrate. The release of the pre-strain mechanically lifts the regions that are not bonded to the substrate to form 3D structures because of the compressive forces (Fig. 1b). When fully bonded, the deformation of the meshed lattice structures in the out-of-plane direction is minimized. The full bonding of wavy meshed ground is applied for easy integration of the antenna on various curvilinear surfaces in the following studies unless otherwise specified. An inset microstrip line with a characteristic impedance of 50 Ω is then used to feed the stretchable microstrip patch antenna. Compared to the probe feeding [31], this in-plane feeding provides easy integration with other COTS chips and electrical components. Although the mechanical properties (e.g., stress–strain curve and stretchability) of the horseshoe unit cells and resulting lattice structures have been shown to depend on the characteristic dimensions, the effect of the orientation of the square lattice with respect to the feeding direction on the mechanical and radiation properties is yet to be investigated. After revealing the orientation effect, the stretchable antennas with mechanically assembled lattice structures are then reported. The tunable mechanicalelectromagnetic properties allow the stretchable microstrip antenna to be designed with strain-sensitive or strain-insensitive properties, with the former for wireless strain sensing and the latter for wireless on-body communication.

3.1 Meshed Microstrip Antennas for Wireless Strain Sensing

Because the square has rotational symmetry of order 4, this work considers three representative orientations (i.e., 0° , 30°, and 45°) (Fig. 2a). The geometric parameters of horseshoe unit cells remain unchanged in the study of orientation effects (i.e., line width w = 0.2 mm, arc radius R = 0.6 mm, and arc angle $\alpha = 180^{\circ}$). The microstrip antenna with a solid patch and ground is designed to resonate at 2.4 GHz. Replacing the solid patch and ground with horseshoe square lattice structures (i.e., the stretchable meshed microstrip antenna in Fig. 2b) lead to the shift of the resonance frequency to a lower value (Fig. S1), which is consistent with the previous report [18, 42]. Though the apparent physical dimensions of the microstrip antennas with horseshoe square lattice structures are not changed from their solid counterparts, the horseshoe lattice structures increase the equivalent wavelength in the current path. According to the cavity model [43], the increased effective dimension of the cavity from the increased current path results in a reduced resonance frequency. The meshed microstrip antenna with an orientation of 30° or 45° direction exhibits a slightly higher resonance

257

258

259

260

261

262

263

264

265

266

267

268

269

271

272

273

274

275

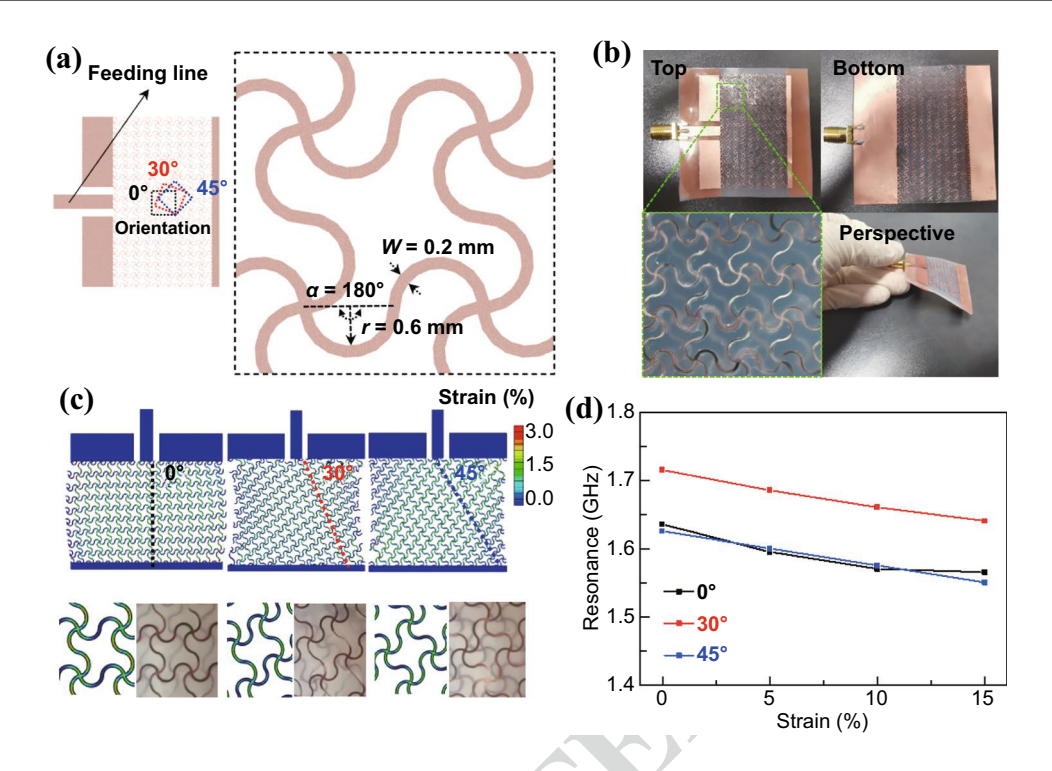


Fig. 2 Mechanical-electromagnetic properties of the meshed microstrip antenna. a Schematic to show the meshed patch composed of horseshoe unit cells in a meshed layout with three different orientations (0°, 30°, and 45°) relative to the feeding line. **b** Optical images of the meshed microstrip antenna with the 0° orientation. c Strain distributions in the meshed patch with different orientations upon 15% stretching. Optical images of the meshed patch upon a tensile strain of 15% from the experiment are included for comparison. d Measured resonance frequency of the meshed microstrip antennas with three different orientations as a function of the applied tensile strain

frequency than that with the 0° orientation before stretching, likely due to the different current distributions in the meshed patch. Although the horseshoe unit cells unravel upon stretching, they unfold differently in the square lattice structure with different orientations. The horseshoe unit cells simultaneously rotate to align and unravel along the stretching (i.e., feeding) direction in the stretchable antenna with the 30° and 45° orientation, whereas the ones in the stretchable antenna with 0° orientation only exhibit unraveling (Figs. 2c and S1a). The predictions from the design by the finite element analysis (FEA) simulation are also verified by the experimental observations. Owing to the additional rotation, the stretchable antenna with the 30° or 45° orientation shows a smaller maximal strain of 2.3% or 2.1% in the horseshoe units of the patch than that of 3.0% in the 0° direction for stretching of 15%. As the maximum strain is below the fracture strain of Cu, the antennas can be further stretched.

Next, the coupled mechanical-electromagnetic properties of the stretchable microstrip antenna are measured to explore their potential for wireless sensing. The reflection coefficient (i.e., the S_{11} value) of the antenna is related to the input impedance (Z) as $S_{11} = 20 \log_{10} |(Z - Z_0)/(Z + Z_0)|$, where Z_0 is the port impedance of 50 Ω . The input impedance of microstrip antennas is a function of feeding location, which is approximately expressed as $Z = \cos^2(\pi x/L)Z(x=0)$, where L is the length of antennas along the feeding direction, x is the inset length, and Z(x = 0) is the input impedance of antennas with feeding on the edge. It should be noted that Z(x = 0) depends on the dimension of antennas and is usually larger than 50 Ω . As the input impedance decreases as the inset length x increases, an optimal inset length can be obtained to match the 50 Ω port. Even though the impedance matching is optimized for the solid microstrip antenna, the small S_{11} values of the stretchable meshed microstrip antennas imply that a good impedance matching is still achieved. Further improvement on impedance matching is also possible with the optimization of the inset length. The resonance frequency f of the patch antenna is inversely proportional to its effective length L_{eff} [44] as:

276

277

278

279

280

281

282

283

284

285

286

287

288

289

290

291

292

293

294

295

(1)

344

345

346

347

348

349

350

351

352

353

354

355

356

357

358

359

360

361

362

363

364

365

366

367

368

369

370

371

372

373

374

375

376

377

378

379

380

381

382

383

384

385

386

387

388

297 298 299

316

317

318

319

320

321

322

323

324

325

326

327

328

329

330

331

332

333

334

335

336

337

338

339

340

341

342

343

 $f = \frac{c}{2L_{\rm eff}\sqrt{\varepsilon_{\rm eff}}},$ where c is the speed of light and $\varepsilon_{\mathrm{eff}}$ is the effective dielectric constant. The effective length is related to the dimension of the patch along the feeding direction with an additional fringing effect for solid microstrip antennas. Owing to the change in the current path, the horseshoe unit cells increase the effective length. The unfolding of the horseshoe unit cells leads to increased effective length and decreased resonance frequency for all three orientations (Figs. 2c and S1). Because of the increased contribution from rotation, the stretchable antenna with the orientation of 30° or 45° exhibits a more linear change in the resonance frequency than the one with the 0° orientation. Compared to the R^2 value of 0.8996 in the linear fitting for the stretchable antenna with the orientation of 0°, the ones with the orientation of 30° (or 45°) showcase a value of 0.999 (or 0.991). The demonstrated linearity in the stretchable antennas is significantly higher than the previous literature reports [31], which is highly desirable for wireless strain sensing or on-body detection of human motions due to the simple calibration. The improved linearity is likely attributed to the additional rotation in the lattice structure during the unraveling process. As shown in Movie S1, the stretchable antenna measures the average mechanical stretching in the antenna from the resonance shift, demonstrating its potential as a wireless strain sensor with the shift to be obtained from remote interrogation. It is also noted that a more uniform deformation to ensure the linearity in the strain sensing can be achieved by a selective bonding only at two ends and/or the use of smaller antennas with higher working frequencies. Compared to the resistive or capacitive strain sensors, the antenna-based wireless strain sensor is of high interest in remoting sensing without wired connections or a power supply. Though wireless strain sensing based on inductive coils has been demonstrated [45], its limited working distance of 2–3 cm can be largely extended to meters with the antenna-based strain sensors. Similar to the previous report [46], the mesh structure slightly decreases the bandwidth of the microstrip antenna from 3% in the solid ones to 1.9–2.8%

3.2 Hierarchically Structured Microstrip Antennas from Mechanical Assembly

ing in a predetermined frequency band.

To reduce the change in resonance frequency upon stretching, the hierarchically structured stretchable antennas

in the ones with three different mesh orientations, featuring

a narrow bandwidth for sensitive strain sensing. Despite the

promising application in sensing, the stretchable microstrip

antenna with a narrow bandwidth and large resonance shift is

not suitable for wireless communication or RF energy harvest-

with mechanically assembled 3D structures are exploited (Fig. 3a). Because the mechanically assembled 3D structures largely depend on the level of pre-strain and strategic bonding sites, these two important factors will be investigated in this section. The former includes the study of three pre-strain levels (i.e., 5%, 10%, and 15%), whereas the latter explores selective bonding either at two ends or with an additional center bonding to induce a single- or double-arch structure. As the stretchable antenna with the 0° orientation is associated with a smaller resonance frequency change upon stretching, it is explored in the following studies unless otherwise specified.

The introduction of the 3D pop-up structure further reduces the resonance frequency of the microstrip antenna (Figs. 3b and S2a-c). The air gap between the 3D structure and substrate results in an increased dielectric layer thickness and decreased dielectric constant. According to the transmission line model, the decrease in the dielectric constant leads to an increased resonance frequency, whereas the increase in the dielectric layer thickness results in a decreased resonance frequency through an increased effective length from the fringing effect. However, the influence from the increased thickness on the resonance frequency dominates over that from the reduced dielectric constant to ultimately result in a reduced resonance frequency in the hierarchically structured stretchable antennas. For instance, the resonance frequency is reduced from 1.63 to 1.45 GHz for a pre-strain of 5% before stretching. The arch height increases from 5 to 8.5 mm as the pre-strain increases from 5 to 15% (Fig. S2a), and it slowly decreases with the stretching level at the beginning and then rapidly afterward. For example, for a pre-strain of 15%, the arch height decreases by 1.5 mm upon 5% strain, then by 2.5 mm upon another successive 5% strain, and finally by 4.5 mm with an additional 5% strain. When tensile strain is applied, the hierarchically structured stretchable antenna reveals an "ordered unraveling", in which the 3D structure arch unravels first to flat and then the horseshoe unfolds (Fig. 2b and Movie S2). The transition between the first and second unraveling occurs when the tensile strain is equal to the pre-strain. The ordered unraveling not only contributes to improved stretchability, but also results in a smaller change in the resonance frequency as it increases in the first unraveling and then decreases in the second (Figs. 3c and S2b-d). In the first unraveling phase, the initial slow increase in the resonance frequency

391

392

393

394

395

396

397

398

399

400

401

402

403

404

405

406

407

408

409

410

(c)

(a)

Pre-strain -5% -10% -15%

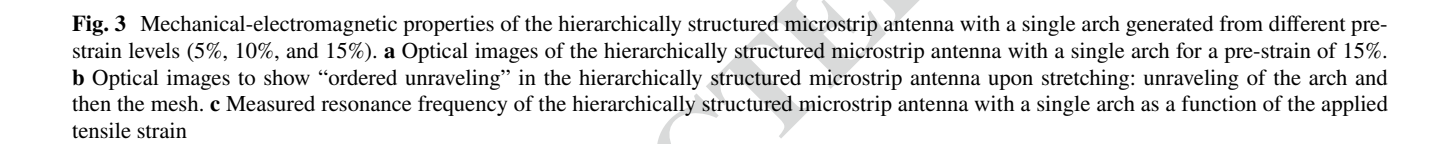
20

25

10

Strain (%)

15



is followed by a rapid increase because of the rapid shape change in the 3D arch (revealed in its measured height, Fig. S2a) near the full unraveling, which is consistent with our prior study [18]. However, the resonance frequency increase in the first unraveling phase is still too large. It is also worth pointing out that the high S_{11} values imply a degraded impedance matching, but it can be improved with a dense mesh or by an optimized inset location in future studies. After the patch and ground plane are fully bonded to a pre-strained (10%) substrate, the release of the pre-strain results in the stretchable microstrip antenna with a wavy patch and ground (Fig. S3a). Different from the arched microstrip antenna, the resonance frequency of the stretchable microstrip antenna with a wavy patch and ground decreases monotonously from 1.73 to 1.65 GHz as the tensile strain increases from 0 to 20% due to the flattening of wavy structures and unfolding of serpentine networks (Fig. S3b).

With an additional center bonding, a double-arched patch in the hierarchically structured stretchable antenna (Fig. 4a) effectively reduces the change in dielectric

constant and dielectric layer thickness for a significantly reduced resonance frequency variation (Fig. 4b-d). It should be noted that the inset length in the hierarchically structured stretchable antenna is optimized to improve impedance matching in case of poor impedance matching. The resonance increase of 0.02 GHz in the double-arched microstrip antenna (Fig. 4e, f) in the first unraveling phase is much smaller than that of 0.12 GHz in its single-arched counterpart (Figs. 3c and S2d) for a pre-strain of 15%. Upon further stretching, the resonance frequency recovers to its initial value to provide an almost unchanged resonance frequency (i.e., < 2% change) over the tensile strain range of 25%. The almost unchanged S_{11} curve upon stretching contributes to an operational band of 0.1 GHz (shadow region in Fig. 4e). Although a similar trend is also observed for a pre-strain of 5% or 10%, the resonance frequency variation is much larger than that of 15%. Compared to the arch height of 8.5 mm in the single-arched design for a pre-strain of 15%, the reduced arch height of 5 mm in the double-arched structure helps to improve the stability of the hierarchically structured microstrip



411

412

413

414

415

416

417

418

419

420

421

422

423

424

425

426

427

428

429

430

431

Article No: 631

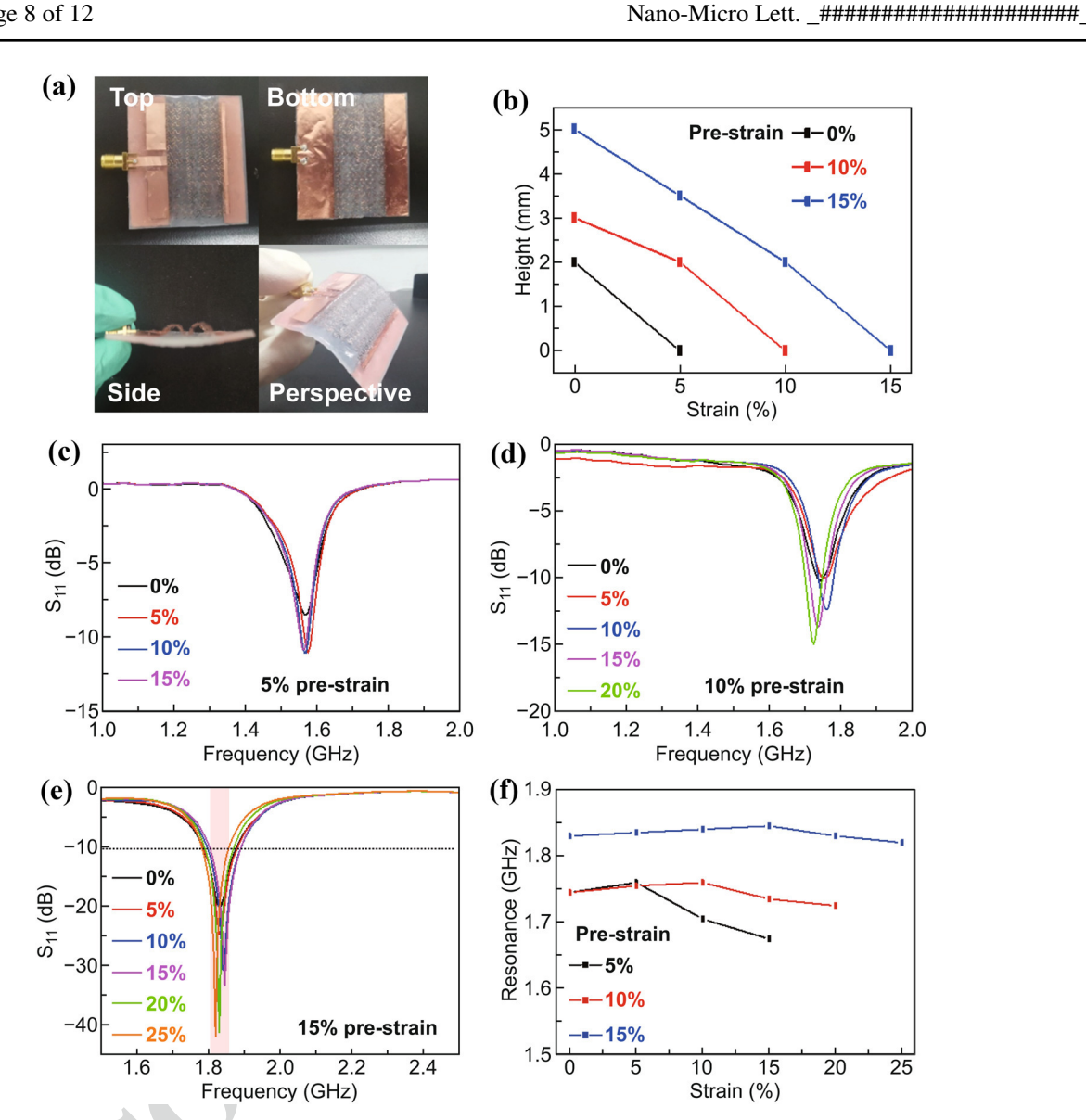


Fig. 4 Strain-insensitive hierarchically structured microstrip antennas with a double-arched patch. **a** Optical images of the strain-insensitive hierarchically structured microstrip antenna with a double-arched patch generated from a pre-strain of 15%. **b** Arch height (or half of the amplitude) as a function of the applied tensile strain. \mathbf{c} - \mathbf{e} Mechanical-electromagnetic properties of the hierarchically structured microstrip antennas with a double-arched patch for a pre-strain of \mathbf{c} 5%, \mathbf{d} 10%, and \mathbf{e} 15% upon stretching. The operational band with the reflection coefficient (S_{11}) less than – 10 dB is shaded in pink. \mathbf{f} Measured resonance frequency of the hierarchically structured microstrip antennas with a double-arched patch upon stretching to highlight the strain-insensitive property in the one from a pre-strain of 15%

antennas upon external perturbations. The smaller air gap in the double-arched microstrip antenna also exhibits improved impedance matching over its single-arched counterpart. Further reduction in the arch height and enhanced impedance matching can be achieved with more selective bonding sites to induce more arches.

In addition to stretching, the double-arched microstrip antenna with a pre-strain of 15% also showcases stable electromagnetic properties (e.g., resonance frequency and radiation patterns) upon bending deformations. With a custom-built bending testing setup (Fig. S4a), the resonance frequency only shows a negligibly small change of $0.012~\rm GHz$ (0.7%) as the double-arched microstrip antenna is bent over a radius of $14.32~\rm mm$ (Fig. S4b, c). After 500 bending cycles applied to the double-arched microstrip antenna, no obvious changes are observed in the structure (Fig. S5a) or S_{11} curves (Fig. S5b), indicating the good mechanical robustness of the stretchable antenna. Compared to the ungrounded antennas

432

433

434

435

436

437

438

439

440

441

442

443

444

445

446

447

448

449

469

470

471

472

473

474

475

476

477

478

479

480

481

482

483

484

485

486

487

488

464

465

466

467

450

451

452

453

454

455

456

457

458

459

(e.g., monopole, dipole, or loop antenna), the stretchable microstrip antenna with a ground plane exhibits excellent on-body performance. Attaching the double-arched microstrip antennas to different parts of the human body measures its on-body performance (Fig. S6a). A small resonance frequency difference of less than 0.04 GHz is observed between the on-body and off-body measurements (Fig. S6b), indicating the effectiveness of the meshed ground.

3.3 Wireless Communication Performance of the Double-arched Microstrip Antennas

The strain-insensitive electromagnetic property of the stretchable microstrip antennas in the intrinsically narrow bandwidth is highly desirable for stable wireless communication and effective RF energy harvesting, especially for on-body applications. Because 2.40–2.48 GHz is a widely used frequency range in wireless communication (e.g., Bluetooth and Wi-fi), the stretchable antennas with a stable resonance frequency around 2.45 GHz can be

directly leveraged for wireless data transmission or powering. The double-arched microstrip antenna with a prestrain of 15% can be easily attached to the curvilinear surface of human arms without causing discomfort (Fig. 5a). Improved adhesion between the antenna and arm can be achieved by coating a thin adhesive Silbione layer on the wavy ground. Because of the reduced antenna dimension from 43.9×35.5 to 31.9×25.5 mm² along with the inset length optimization, the double-arched microstrip antenna resonates at 2.45 GHz, as confirmed by the experimental measurements (Fig. 5b). The negligibly small influence of human bodies on the resonance frequency of the antenna also demonstrates the effectiveness of the meshed ground in this new design. Further improvement in the on-body performance (e.g., screening effect and radiation directionality) can be achieved with a dense ground mesh.

The wireless communication performance of the double-arched microstrip antenna is measured with a commercial RF evaluation kit consisting of a transmitter and a receiver (SmartRF06) (Fig. S7). The transmitter integrated with a PCB-based omnidirectional antenna and a CC2538

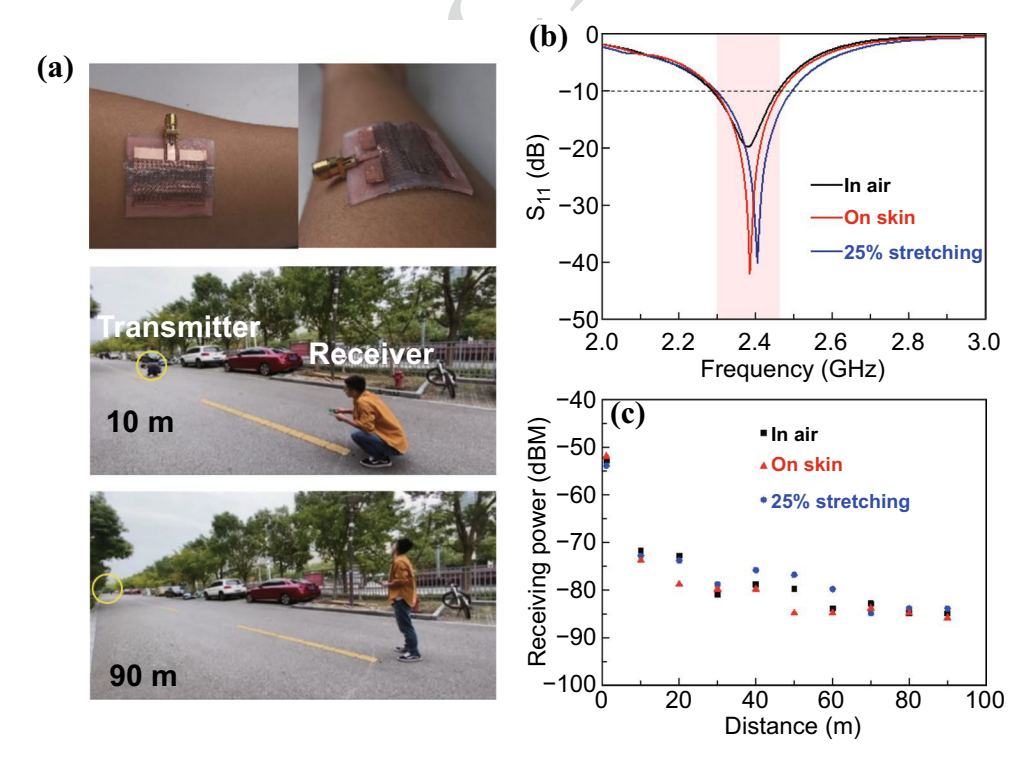


Fig. 5 Wireless communication performance of the strain-insensitive hierarchically structured microstrip antenna resonating at 2.4 GHz. a Optical images of the strain-insensitive hierarchically structured microstrip antenna conformally attached to the human arm and the experimental setup to evaluate its wireless communication performance. b Measured S_{11} curves of the strain-insensitive hierarchically structured microstrip antenna in free-space or on the human arm with/without a tensile strain of 25%. c Measured receiving power by the strain-insensitive stretchable antenna from a transmitter positioned at different distances



534

535

536

537

538

539

540

541

542

543

544

545

546

547

548

549

550

551

552

553

554

555

556

557

558

559

560

561

562

563

564

565

566

567

568

569

570

571

572

573

574

575

576

577

578

579

580

581

489

490

505

506

507

508

509

510

511

512

513

514

515

516

517

518

519

520

521

522

523

524

525

526

527

528

529

530

531

RF chip is programmed to transmit RF power at -3 dBm (0.50 mW). The receiver with a sensitivity of -100 dBmis integrated with the double-arched microstrip antenna. The stretchable microstrip antenna was either placed in the air or on the human skin and upon mechanical stretching. The communication performance is evaluated in the open space at a university campus (Fig. 5a). Although the receiving power decreases rapidly with the communication distance for both the in-air and on-skin case, the receiver is still able to receive - 100 dBm at a distance of ~ 100 m (Fig. 5c). It is believed that the working distance can be improved further by increasing the transmitting power of the source. The stretchable microstrip antenna in this work exhibits improved communication performance in the free space over the previous demonstrations (e.g., with a stretchable monopole antenna [39]). Compared to the received power of -75 dBm by the monopolar antenna from a 1 dBm transmitter at a distance of 20 m, our stretchable microstrip antennas demonstrate a higher received power of -72 dBm from a transmitter with an even lower power of -3 dBm. Moreover, the significantly enhanced on-body performance of the stretchable microstrip patch antenna further results in a small difference in the receiving power between the on-body and free-space demonstrations. For example, the receiving power difference at a distance of 20 m between the "in-air" and "on-body" case is ~ 5 dBm, much lower than that for the monopole antenna (~12 dBm). These improved on-body performance parameters in wireless communication are attributed to the almost unchanged resonance frequency and radiation properties of the stretchable microstrip antenna (Fig. 5b). The wireless communication performance of the stretchable microstrip antenna upon deformations was also investigated. Mechanical stretching leads to a slight change of the receiving power, which can be explained by negligible resonance frequency change of the stretchable microstrip antenna upon stretching.

4 Conclusions

In summary, we have introduced a hierarchically structured stretchable microstrip antenna with horseshoe unit cells arranged in a square lattice structure that is further mechanically assembled into a 3D layout. The resulting stretchable antenna showcases tunable, especially strain-insensitive mechanical-electromagnetic properties with improved overall stretchability. In particular, an almost unchanged resonance frequency with a shift of < 0.02 GHz is demonstrated within the tensile strain range from 0 to 25%. To the best of our knowledge, this is the first demonstrated stretchable microstrip antenna that has almost unchanged resonance frequency over a tensile strain range of over 25%. The stretchable microstrip patch antennas with the strain-insensitive resonance frequency and enhanced stretchability extend their application from wireless sensing to stable on-body wireless communication and effective RF energy harvesting. Additionally, the design approach based on the coupled mechanical-electromagnetic simulations also allows us to identify the stretchable microstrip antennas as wireless sensors with enhanced linearity. This work provides a powerful toolkit with coupled mechanical-electromagnetic simulations and cost-effective manufacturing approaches to design stretchable microwave components/devices for integrated stretchable systems.

Acknowledgements This work was supported by the National Science Foundation (NSF) (Grant No. ECCS-1933072), the National Heart, Lung, And Blood Institute of the National Institutes of Health under Award Number R61HL154215, the International Partnership Program of Chinese Academy of Science. (Grant No.154232KYSB20200016), the Suzhou Science and Technology Support Project (Grant No. SYG201905), the National Key Research and Development Program of China. (Grant No. 2020YFC2007400) and Penn State University. The use of the RF characterization facility provided by Prof. Mehdi Kiani at Penn State University was also acknowledged. Computations for this research were performed on the Pennsylvania State University's Institute for Computational and Data Sciences' Roar supercomputer. J.Z. would like to acknowledge the Leighton Riess Graduate Fellowship and Diefenderfer Graduate Fellowship in Engineering from Penn State University. J.Z. would like to thank helpful discussions with Prof. Michael Lanagan, Prof. Mark Horn, Prof. Xin Ning, Prof. Jian Hsu, and Xianzhe Zhang. S.Z. would like to acknowledge Zhisen Wang, Kun Huang, Benkun Bao, Yingying Zhang, and Qi Lu's help in the design and fabrication of stretcher and wireless communication measurements.

Open Access This article is licensed under a Creative Commons Attribution 4.0 International License, which permits use, sharing, adaptation, distribution and reproduction in any medium or format, as long as you give appropriate credit to the original author(s) and the source, provide a link to the Creative Commons licence, and indicate if changes were made. The images or other third party material in this article are included in the article's Creative Commons licence, unless indicated otherwise in a credit line to the material. If material is not included in the article's Creative Commons licence and your intended use is not permitted by statutory regulation or exceeds the permitted use, you will need to obtain

(https://doi.org/10.1007/

Page 11 of 12 _####_

633

634

635

636

637

638

639

640

641

643

644

645

646

647

648

649

650

651

652

653

654

655

656

657

658

659

660

661

662

663

664

665

666

667

668

669

671

672

673

674

675

676

677

678

679

680

681

682

683

684

685

686

687

582 583

584 585

586

588 589 590

591

587

596

597

603

614

629 630 631

632

Supplementary Information The online version contains supplementary material available at s40820-021-00631-5).

References

1. S. Bauer, Sophisticated skin. Nat. Mater. 12(10), 871-872 (2013). https://doi.org/10.1038/nmat3759

permission directly from the copyright holder. To view a copy of

this licence, visit http://creativecommons.org/licenses/by/4.0/.

- 2. M. Ha, J. Park, Y. Lee, H. Ko, Triboelectric generators and sensors for self-powered wearable electronics. ACS Nano 9(4), 3421-3427 (2015). https://doi.org/10.1021/acsnano.5b01478
- 3. L. Li, Z. Wu, S. Yuan, X.-B. Zhang, Advances and challenges for flexible energy storage and conversion devices and systems. Energy Environ. Sci. 7(7), 2101-2122 (2014). https:// doi.org/10.1039/C4EE00318G
- 4. J.-G. Sun, T.-N. Yang, C.-Y. Wang, L.-J. Chen, A flexible transparent one-structure tribo-piezo-pyroelectric hybrid energy generator based on bio-inspired silver nanowires network for biomechanical energy harvesting and physiological monitoring. Nano Energy 48, 383–390 (2018). https://doi.org/ 10.1016/j.nanoen.2018.03.071
- 5. H. Zhou, Y. Zhang, Y. Qiu, H. Wu, W. Qin et al., Stretchable piezoelectric energy harvesters and self-powered sensors for wearable and implantable devices. Biosens. Bioelectron. 168, 112569 (2020). https://doi.org/10.1016/j.bios.2020.112569
- 6. C. Zhang, Z. Peng, C. Huang, B. Zhang, C. Xing et al., Highenergy all-in-one stretchable micro-supercapacitor arrays based on 3D laser-induced graphene foams decorated with mesoporous ZnP nanosheets for self-powered stretchable systems. Nano Energy **81**, 105609 (2020). https://doi.org/10. 1016/j.nanoen.2020.105609
- 7. Y. Xu, G. Zhao, L. Zhu, Q. Fei, Z. Zhang et al., Pencil-paper on-skin electronics. Proc. Natl. Acad. Sci. USA 117(31), 18292 (2020). https://doi.org/10.1073/pnas.2008422117
- 8. Y. Qiu, Y. Tian, S. Sun, J. Hu, Y. Wang et al., Bioinspired, multifunctional dual-mode pressure sensors as electronic skin for decoding complex loading processes and human motions. Nano Energy 78, 105337 (2020). https://doi.org/10.1016/j. nanoen.2020.105337
- 9. K. Lee, X. Ni, J.Y. Lee, H. Arafa, D.J. Pe et al., Mechanoacoustic sensing of physiological processes and body motions via a soft wireless device placed at the suprasternal notch. Nat. Biol. Eng. 4(2), 148–158 (2020). https://doi.org/10.1038/ s41551-019-0480-6
- 10. Y. Lee, C. Howe, S. Mishra, D.S. Lee, M. Mahmood, M. Piper et al., Wireless, intraoral hybrid electronics for real-time quantification of sodium intake toward hypertension management. Proc. Natl. Acad. Sci. USA 115(21), 5377 (2018). https://doi. org/10.1073/pnas.1719573115
- Q. Pang, D. Lou, S. Li, G. Wang, B. Qiao et al., Smart flexible electronics-integrated wound dressing for real-time monitoring

- and on-demand treatment of infected wounds. Adv. Sci. 7(6), 1902673 (2020). https://doi.org/10.1002/advs.201902673
- 12. S. Wagner, S. Bauer, Materials for stretchable electronics. MRS Bull. 37(3), 207–213 (2012). https://doi.org/10.1557/ mrs.2012.37
- 13. J. Zhu, H. Cheng, Recent development of flexible and stretchable antennas for bio-integrated electronics. Sensors 18(12), 4364 (2018). https://doi.org/10.3390/s18124364
- 14. Y. Liu, X. Wang, Y. Xu, Z. Xue, Y. Zhang et al., Harnessing the interface mechanics of hard films and soft substrates for 3D assembly by controlled buckling. Proc. Natl. Acad. Sci. USA 116(31), 15368 (2019). https://doi.org/10.1073/pnas. 1907732116
- 15. Z. Song, X. Wang, C. Lv, Y. An, M. Liang et al., Kirigamibased stretchable lithium-ion batteries. Sci. Rep. 5(1), 10988 (2015). https://doi.org/10.1038/srep10988
- 16. Z. Yan, F. Zhang, F. Liu, M. Han, D. Ou et al., Mechanical assembly of complex, 3D mesostructures from releasable multilayers of advanced materials. Sci. Adv. 2(9), e1601014 (2016). https://doi.org/10.1126/sciadv.1601014
- 17. T. Chang, Y. Tanabe, C.C. Wojcik, A.C. Barksdale, S. Doshay et al., A general strategy for stretchable microwave antenna systems using serpentine mesh layouts. Adv. Funct. Mater. 27(46), 1703059 (2017). https://doi.org/10.1002/adfm.20170 3059
- 18. J. Zhu, J.J. Fox, N. Yi, H. Cheng, Structural design for stretchable microstrip antennas. ACS Appl. Mater. Interfaces 11(9), 8867-8877 (2019). https://doi.org/10.1021/acsami.8b22021
- Y. Wang, C. Zhu, R. Pfattner, H. Yan, L. Jin et al., A highly stretchable, transparent, and conductive polymer. Sci. Adv. 3(3), e1602076 (2017). https://doi.org/10.1126/sciadv.1602076
- 20. Y.R. Jeong, J. Kim, Z. Xie, Y. Xue, S.M. Won et al., A skinattachable, stretchable integrated system based on liquid gainsn for wireless human motion monitoring with multi-site sensing capabilities. NPG Asia Mater. 9(10), e443 (2017). https://doi.org/10.1038/am.2017.189
- 21. Y. Hu, T. Zhao, P. Zhu, Y. Zhu, X. Shuai et al., Low cost and highly conductive elastic composites for flexible and printable electronics. J. Mater. Chem. C 4(24), 5839–5848 (2016). https://doi.org/10.1039/C6TC01340F
- 22. Z. Huang, Y. Hao, Y. Li, H. Hu, C. Wang et al., Three-dimensional integrated stretchable electronics. Nat. Electron. 1(8), 473-480 (2018). https://doi.org/10.1038/s41928-018-0116-y
- 23. K.-I. Jang, H.U. Chung, S. Xu, C.H. Lee, H. Luan et al., Soft network composite materials with deterministic and bioinspired designs. Nat. Commun. 6(1), 6566 (2015). https:// doi.org/10.1038/ncomms7566
- 24. S. Xu, Y. Zhang, J. Cho, J. Lee, X. Huang et al., Stretchable batteries with self-similar serpentine interconnects and integrated wireless recharging systems. Nat. Commun. 4(1), 1543 (2013). https://doi.org/10.1038/ncomms2553
- 25. F. Liu, Y. Chen, H. Song, F. Zhang, Z. Fan et al., High performance, tunable electrically small antennas through mechanically guided 3D assembly. Small 15(1), 1804055 (2019). https://doi.org/10.1002/smll.201804055



731

732

733

734

735

736

737

738

739

740

741

742

743

744

745

746

747

748

749

750

751

752

753

754

755

756

757

758

759

760

761

762

763

764

765

766

767

768

769

688

689

690

691

692

693

694

695

696

697

698

699

700

701

702

703

704

705

706

707

708

709

710

711

715

716

717

718

719

720

721

722

723

724

725

726

727

728

729

26. H.U. Chung, B.H. Kim, J.Y. Lee, J. Lee, Z. Xie et al., Binodal, wireless epidermal electronic systems with in-sensor analytics for neonatal intensive care. Science 363(6430), eaau0780 (2019). https://doi.org/10.1126/science.aau0780

Article No: 631

- 27. M. Zulgarnain, S. Stanzione, G. Rathinavel, S. Smout, M. Willegems et al., A flexible ECG patch compatible with NFC RF communication. NPJ Flex. Electron. 4(1), 13 (2020). https:// doi.org/10.1038/s41528-020-0077-x
- 28. J. Kim, A. Banks, Z. Xie, S.Y. Heo, P. Gutruf et al., Miniaturized flexible electronic systems with wireless power and nearfield communication capabilities. Adv. Funct. Mater. 25(30), 4761-4767 (2015). https://doi.org/10.1002/adfm.201501590
- 29. Y. Luo, L. Pu, G. Wang, Y. Zhao, RF energy harvesting wireless communications: Rf environment, device hardware and practical issues. Sensors 19(13), 3010 (2019), https://doi.org/ 10.3390/s19133010
- 30. A.N. Parks, A.P. Sample, Y. Zhao, J.R. Smith, A wireless sensing platform utilizing ambient RF energy. 2013 IEEE Topical Conference on Biomedical Wireless Technologies, Networks, and Sensing Systems. 154-156 (2013)
- 31. Y.-S. Kim, A. Basir, R. Herbert, J. Kim, H. Yoo et al., Soft materials, stretchable mechanics, and optimized designs for bodywearable compliant antennas. ACS Appl. Mater. Interfaces 12(2), 3059–3067 (2020), https://doi.org/10.1021/acsami.9b20233
- 32. S. Cheng, Z. Wu, A microfluidic, reversibly stretchable, large-712 area wireless strain sensor. Adv. Funct. Mater. 21(12), 2282-713 2290 (2011). https://doi.org/10.1002/adfm.201002508 714
 - 33. S. Cheng, Z. Wu, P. Hallbjorner, K. Hjort, A. Rydberg, Foldable and stretchable liquid metal planar inverted cone antenna. IEEE Trans. Antennas Propag. **57**(12), 3765–3771 (2009). https://doi.org/10.1109/TAP.2009.2024560
 - 34. G.J. Hayes, J. So, A. Qusba, M.D. Dickey, G. Lazzi, Flexible liquid metal alloy (EGaln) microstrip patch antenna. IEEE Trans. Antennas Propag. **60**(5), 2151–2156 (2012). https:// doi.org/10.1109/TAP.2012.2189698
 - 35. M. Stoppa, A. Chiolerio, Wearable electronics and smart textiles: a critical review. Sensors 14(7), 11957-11992 (2014). https://doi.org/10.3390/s140711957
 - 36. K. Pan, Y. Fan, T. Leng, J. Li, Z. Xin et al., Sustainable production of highly conductive multilayer graphene ink for wireless connectivity and loT applications. Nat. Commun. 9(1), 5197 (2018). https://doi.org/10.1038/s41467-018-07632-w

- 37. M. Kubo, X. Li, C. Kim, M. Hashimoto, B.J. Wiley et al., Stretchable microfluidic radiofrequency antennas. Adv. Mater. 22(25), 2749–2752 (2010). https://doi.org/10.1002/adma. 200904201
- 38. T. Rai, P. Dantes, B. Bahreyni, W.S. Kim, A stretchable RF antenna with silver nanowires. IEEE Electron. Devices Lett. 34(4), 544–546 (2013). https://doi.org/10.1109/LED.2013. 2245626
- 39. A.M. Hussain, F.A. Ghaffar, S.I. Park, J.A. Rogers, A. Shamim et al., Metal/polymer based stretchable antenna for constant frequency far-field communication in wearable electronics. Adv. Funct. Mater. 25(42), 6565–6575 (2015). https://doi.org/ 10.1002/adfm.201503277
- 40. F.A. Tahir, A. Javed, A compact dual-band frequency-reconfigurable textile antenna for wearable applications. Microw. Opt. Tech. Lett. 57(10), 2251–2257 (2015). https://doi.org/ 10.1002/mop.29311
- 41. A. Michel, R. Colella, G.A. Casula, P. Nepa, L. Catarinucci et al., Design considerations on the placement of a wearable UHF-RFID PIFA on a compact ground plane. IEEE Trans. Antennas Propag. 66(6), 3142-3147 (2018). https://doi.org/ 10.1109/TAP.2018.2811863
- 42. R. Quarfoth, Y. Zhou, D. Sievenpiper, Flexible patch antennas using patterned metal sheets on silicone. IEEE Antennas Wireless Propag. Lett. 14, 1354–1357 (2015). https://doi.org/ 10.1109/LAWP.2015.2406887
- 43. Y. Lo, D. Solomon, W. Richards, Theory and experiment on microstrip antennas. IEEE Trans. Antennas Propag. 27(2), 137-145 (1979). https://doi.org/10.1109/TAP.1979.1142057
- 44. J. Kurian, U. R. M.N, S.K. Sukumaran, Flexible microstrip patch antenna using rubber substrate for WBAN applications. IEEE 2014 International Conference on Contemporary Computing and Informatics (IC3I). 983–986 (2014)
- 45. R. Lin, H.-J. Kim, S. Achavananthadith, S.A. Kurt, S.C.C. Tan et al., Wireless battery-free body sensor networks using near-field-enabled clothing. Nat. Commun. 11(1), 444 (2020). https://doi.org/10.1038/s41467-020-14311-2
- 46. Q.H. Dao, R. Braun, B. Geck, Design and investigation of meshed patch antennas for applications at 24 GHz. 2015 European Radar Conference (EuRAD). 477-480 (2015).